

Behaviour of Large Cylindrical Offshore Structures Subjected to Wave Loads

Begüm Yurdanur DAĞLI¹, Muhammed Ensar Yiğit¹, Ümit GÖKKUŞ¹

¹*Department of Civil Engineering, Manisa Celal Bayar University, Manisa, TURKEY*

Abstract -Spar-type and monopole substructures consisting of a large-diameter, single vertical cylinders have been used as wind turbine towers, oil storage platforms, tankers and wave energy converters at deepwater region in the sea. These towers and platforms are exposed to environmental forces such as wind, wave and current. Wave force is the most effective force in the total environmental force. The body disturbs the incident wave and Diffraction Theory is used for computing the pressure distribution for designing the structure. Therefore, this study aims to present the effect of structural design of towers on dynamic behavior due to wave actions. Two different cases of structural models are selected to employ bidirectional fluid structure interaction (FSI) analysis. Diffraction Theory is utilized to investigate wave forces. Solid and fluid domains are modeled in Abaqus finite elements program. Behaviors of various types of offshore structures are evaluated and compared according to the significant stresses and displacements. The hydrodynamic pressure on the cylindrical structure surface and the diffraction forces acting on structures are presented. Mode shapes, first three natural frequencies are comparatively given.

Keywords: ABAQUS, diffraction theory, fluid structure interaction, large cylindrical offshore structures

DOI: 10.18421/TEM63-16

<https://dx.doi.org/10.18421/TEM63-16>

Corresponding author: Begüm Yurdanur DAĞLI,
Department of Civil Engineering, Manisa Celal Bayar University, Manisa, TURKEY

Email: begum.dagli@cbu.edu.tr

 © 2017 Begüm Yurdanur DAĞLI, Muhammed Ensar Yiğit, Ümit GÖKKUŞ; published by UIKTEN. This work is licensed under the Creative Commons Attribution-NonCommercial-NoDerivs 3.0 License.

The article is published with Open Access at www.temjournal.com

1. Introduction

Most of offshore structures such as wind turbine towers, oil storage platforms, tankers and wave energy converters are considered as large cylindrical structures. Currently, more than 5,400MW of offshore wind power has been installed, most of which is within a water depth less than 60 m with a fixed bottom supporter, such as a monopole [1]. The oil and gas industry focuses on deep water resources due to the limited hydrocarbon resources within the onshore. In this area spar type platforms are commonly installed for the purpose of oil and gas explorations [2]. In present day, significant research is increasing in ocean wave energy industry with the worlds growing energy demand [3]. Wave energy devices also typically have large supporting structures. Wave force is the most significant force that affects the dynamic responses, contribute about 70% of the total environmental force [2]. A common problem in offshore engineering is to predict the wave forces exerted on offshore structures. The Morison equation, Froude Krylov theory and Diffraction Theory are used to calculate the wave forces acting on offshore structures. Diffraction Theory is applicable for structures that are large compared to water wave length [4]. Wave loads are evaluated by applying potential theory. However, in many studies, Morison equation was used to compute the wave force for large structures. The reason being is because of the ease in use of the Morison equation compared to the Diffraction Theory that is more complicated [2]. The linear hydrodynamic analysis of truss-spar is presented by Mansouri and Hadidi [5]. The wave forces are determined by modified Morison equation and Diffraction Theory and the dynamic behavior is investigated due to random waves. A comparative study is performed by Diffraction Theory subjected to long crested waves and short crested waves to observe the dynamic response of a spar type structure by Kurian et al.[2]. Their study proves that Diffraction Theory is found to be more appropriate for the structures which are large compared to the wave length.

The fluid structure interaction (FSI) techniques are widely used to investigate the dynamic response of structure subjected to the wave forces [6]. FSI analyses can be classified as unidirectional and bidirectional. In unidirectional type, only the fluid effect is taken into consideration, in bidirectional type the fluid and structure fields affect each other [7]. Although FSI analyses are limited by heavy computational requirements the finite element software has a wide range of applications in civil engineering analyses [8-10], as applied in this study.

The effect of structural design on the dynamic behavior of offshore structures subjected to environmental loads has been examined in the present paper. Only wave loads are adopted as environmental loads. A first-order analytical solution is introduced for the problem of wave diffraction around a submerged cylindrical structure. Using the body surface boundary conditions and matching outside flow for the determination of unknown coefficients of the series. The velocity potential, and consequently the exciting forces are obtained by solving equations. This paper investigates the effects of wave forces in 20m (d) depth by Diffraction Theory. Incident wave direction is set lateral to detect effects on structural behavior of models. In this study two different cases of structural model are analyzed to provide effective design. Geometrically and materially linear steel shell model is used as a first model (Case I) for dynamic analysis. The second model (Case II) consists of extra plates which are used for strengthening of thin-walled steel structures against local buckling. The diameter is considered as 4.0m (D) for both models. In order to verify the effect of wall thickness (t_w) on Von Mises stresses, four values of $t_w=0.003, 0.005, 0.007$ and 0.010 m are assumed. Numerical simulations are also applied by using a 3D finite-element model within the framework of ABAQUS [11] via FSI. Bidirectional FSI analysis, which is difficult to apply because of heavy computational requirements, has been performed on two different structural models. The application of FSI analysis under the wave forces defined by complex Diffraction Theory makes the study realistic and original. Eight analyses are performed by matching two structural models with different wall thickness. The variations of displacements, Von Mises stress values are compared and the wall thickness is optimized based on the buckling checks.

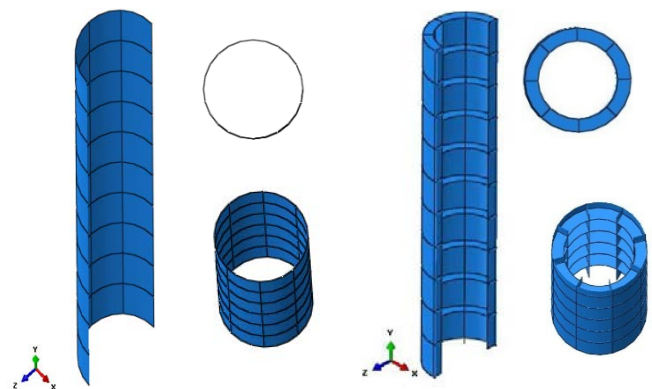
2. Material and method

The models are composed of fluid and structure domains that interact with one another. Two different cases of structural models are investigated to determine optimal shape design via a nonlinear numerical model using the ABAQUS analysis program. The structures are modeled by circular cylinder which is one of the popular geometries of offshore structures [4]. The submerged cylindrical structures selected for this study have heights (h) of 20m. The radius is considered as 2.0m (a) for both cases. The hydrodynamic wave forces are presented by Diffraction Theory.

In FSI analysis, the structures are described by finite-element meshes. The external surface of the finite-element mesh is used as a boundary for the fluid flow. In this way, the contact surfaces where the forces transfer from fluid to structure, and where deformations transfer from structure to fluid, are determined.

2.1. Structural domain

In this study two different cases of structural model are examined, as shown in Figure 1. Linear



steel shell model is used as a first case (Case I) and the second case (Case II) consists of extra plates which are used for strengthening of thin-walled steel structures.

(a) Case I (b) Case II
Figure 1. Case configurations for cylindrical structure models

The structures composed by uniform and homogeneous material are designed under assumption that they are fixed to sea bed. The value for the Young modulus of steel is considered to be $21 \times 10^7 \text{KN/m}^2$. For steel, it is assumed that the material would obey Von Mises' yield criterion with the associated Prandtl-Reuss flow rule [12]. The value of Poisson's ratio is 0.3 and density is 78.50KN/m^3 . The heights of the submerged

cylindrical structures are 20m. In order to optimize structural design, four values of $t_w=0.003, 0.005, 0.007$ and 0.010m are taken into account as wall thicknesses for each case. In Case II the horizontal reinforcement ring on the cylindrical shell is 0.50m in length. The cylindrical shell structure is configured with vertical reinforcement which is of $0.06 \times 0.50\text{m}$ rectangular flat-plate. The dead weight and environmental loads including wave loads in the global x direction are considered in structural analysis.

2.2. Fluid domain

Hydrodynamic wave pressures acting on cylindrical structure are calculated using wave parameters. The wave height H, wavelength L and wave period T are major wave parameters that must be considered in the design of any offshore facilities [13-14]. Also water depth d is an essential parameter to determine the wave theories which are applicable to different environmental conditions [15]. In this study the parameters are taken into account as $H=2.0\text{m}, T=6\text{s}, L=15\text{m}, d=20\text{m}$ and the response of the seabed is neglected. The properties of fluid are chosen to characterize the sea water, with the density of 1025kg/m^3 and the dynamic viscosity of 0.0015Ns/m^2 . The analysis is based on the boundary condition applied to fluid domain as fluid inlet pressures that represent the Diffraction Theory as given below [16]

$$p = \frac{\rho g H \cosh(k(z+d))}{\pi k a \cosh(kd)} \sum_{p=0}^{\infty} \frac{i\beta_p}{H_p^{(1)'}(ka)} \cos(p\theta) e^{-i\omega t} \quad (1)$$

Where ρ is density, g is the gravity, $i = \sqrt{-1}$, $H_p^{(1)'}(kr)$ is Hankel function of the first kind of order p , H is wave height and k is the wave number, which is linked with the wave frequency ω .

The structure of the radius a , is submerged in water of the finite depth d . The rectangular coordinate system (x, y, z) is assumed in which the x - y axes lie on the undisturbed free surface and the z axis is vertically upwards. And

$$\beta_p = \begin{cases} 1 & p=0 \\ 2i^p & p \geq 1 \end{cases} \quad (2)$$

The surface profile is defined in respect to the velocity potential as [17]

$$\eta = i \frac{H}{2} \sum_{p=0}^{\infty} \beta_p \left[J_p(kr) - \frac{J_p'(ka)}{H_p^{(1)'}(ka)} H_p^{(1)}(kr) \right] \cos(p\theta) e^{-i\omega t} \quad (3)$$

where $J_p(kr)$ is Bessel function of p th order with respect to argument (kr) .

The water surface variations are presented at angles of $0^\circ, 90^\circ, 180^\circ$ and 270° in the longitudinal direction due to diffraction of incident wave during the period, in Figure 2.

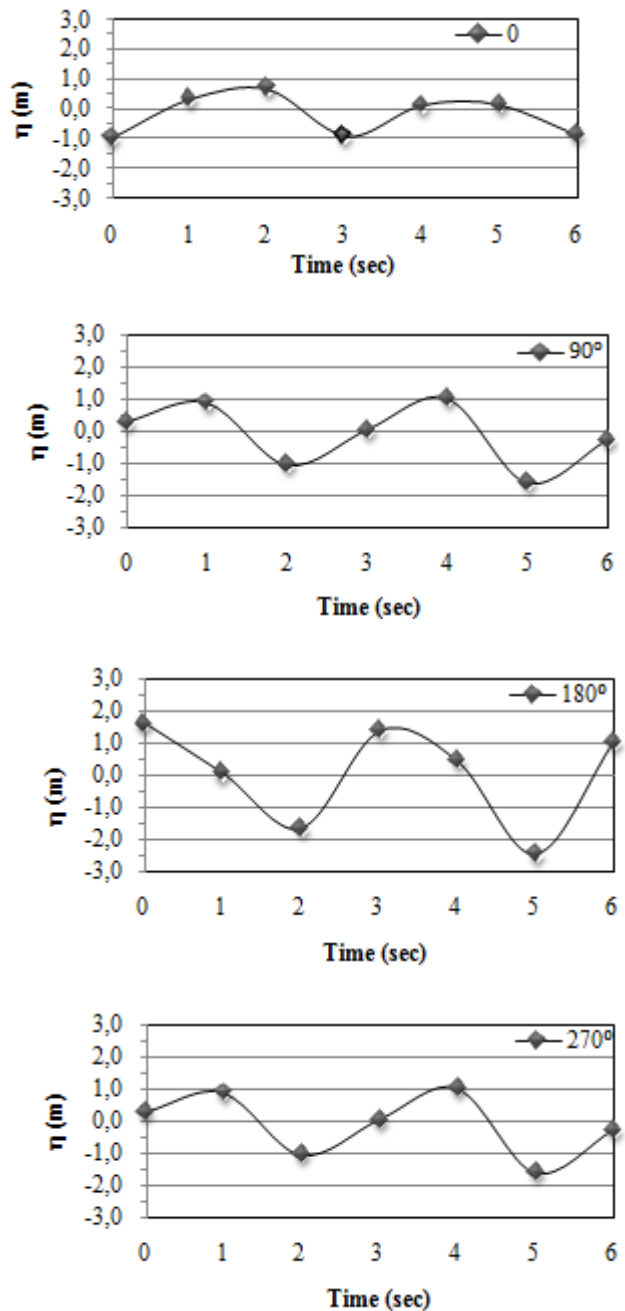


Figure 2. Water surface profiles

2.3. Coupled fluid-structure interaction system

Offshore fluid domain occurs from water domain and cylindrical structure constitutes the solid domain, as given in Figure 3. The dimensions of the water domain are 10m x 10m x 20m in directions x, z, y respectively. The flow around the large cylindrical offshore structure is modeled by CFD technique.

Two-way FSI co-simulation with Fluent CFD-code and Abaqus structural FEM (Finite Element Method)-code is applied successfully. For flow around the large cylindrical tower and the following boundary conditions are shown in Figure 3.

The surface defined as fluid inlet, is divided in 10 sectors. For each sector, the pressure is assigned by keeping the distance from the center of a sector to seabed, constant. The hydrodynamic pressure varies by time at the inlet boundary as shown in Eq. (1).

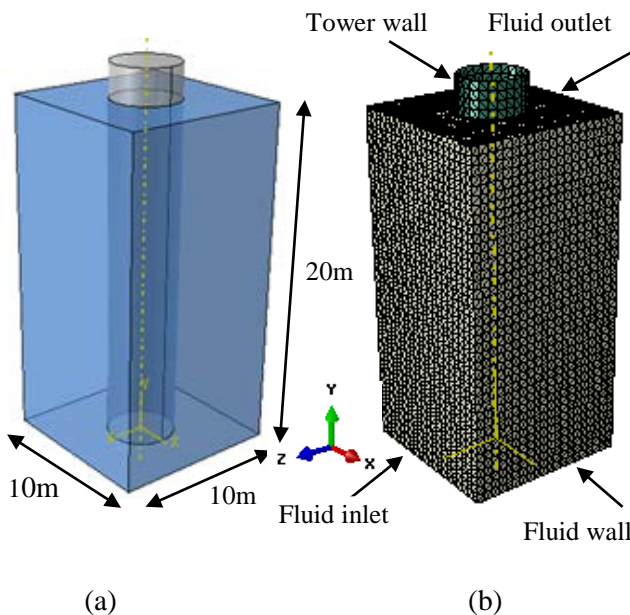


Figure 3. (a) Unmeshed domains (b) Meshed domains

The streamwise variation for pressure components is set as zero at the outlet boundary. The non-slip wall boundary condition is considered at the bottom surface. The salty water properties are assigned for fluid which is modeled as EOS material. The models are cut into several small elements to apply FEM [18]. The volume of the fluid domain includes 4- node modified tetrahedron elements (FC3D4) around the members to solve the boundary layer more efficiently and refined mesh contains 829629 elements for Case I and 1029629 elements for Case II. The deformations caused by hydrodynamic forces are conveyed from structure to

fluid. This cycle runs through the analysis and can be defined as follows

$$m^{Ni} \ddot{u}^N |_t = (F^i - K^i) |_t \quad (4)$$

Where m^{Ni} , K^i are the mass matrix and the internal force vector. The external force obtained from CFD analysis, is defined by F^i and the acceleration is symbolized by \ddot{u}^N . The explicit time integration scheme is presented for solution of displacement problems.

To compute the numerical derivative of a function, central-difference integration method is used [19]. The central difference rules can be generated using the definition given as follows

$$\begin{aligned} \dot{u}^N \left(i+\frac{1}{2} \right) &= \dot{u}^N \left(i-\frac{1}{2} \right) + \frac{\Delta t_{(i+1)} + \Delta t_{(i)}}{2} \ddot{u}^N_{(i)} \\ u^N_{(i+1)} &= u^N_{(i)} + \Delta t_{(i+1)} \dot{u}^N \left(i+\frac{1}{2} \right) \end{aligned} \quad (5)$$

Where u^N refers degree of freedom of displacement component, i is the increment number operator and $(\dot{})$ denotes derivative with respect to time. The cylindrical structures (for Case I and Case II) are discomposed into 10 sections to assign different values of hydrodynamic pressure, as shown in Figure 4.

Fluid pressures are transferred to structure and applied as distributed loads. The models are cut into several elements in the finite elements method which uses the equation of motion given as

$$[m]\{\ddot{u}\} + [c]\{\dot{u}\} + [k]\{u\} = F(t) \quad (6)$$

Here m is the mass matrix, c is the damping matrix and k is the stiffness matrix of the model. At the same equation displacement, velocity, and acceleration vectors are presented by u, \dot{u}, \ddot{u} respectively.

Eight analyses are performed by matching two structural models, using the Abaqus - two way FSI analysis.

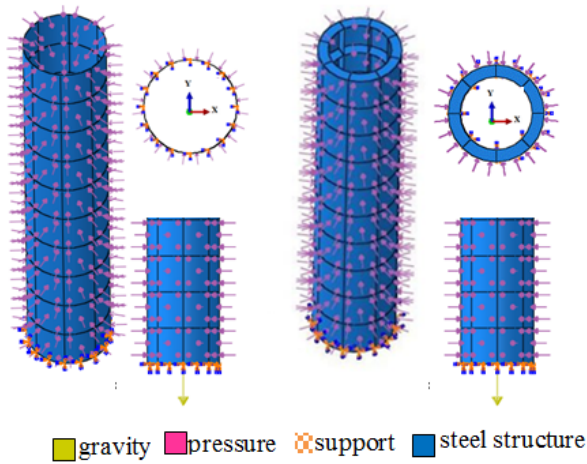


Figure 4. Discomposed sections of cylindrical structures

3. Numerical results

The large cylindrical structures are examined on two different models (Case I and Case II) to provide a more accurate and effective design under diffracted wave loadings. The Diffraction Theory is employed to observe the pressure distribution on cylindrical structure surface at angles of 0° , 45° , 90° , 135° , 180° , 225° , 270° and 315° in the longitudinal direction shown as Figure 5.

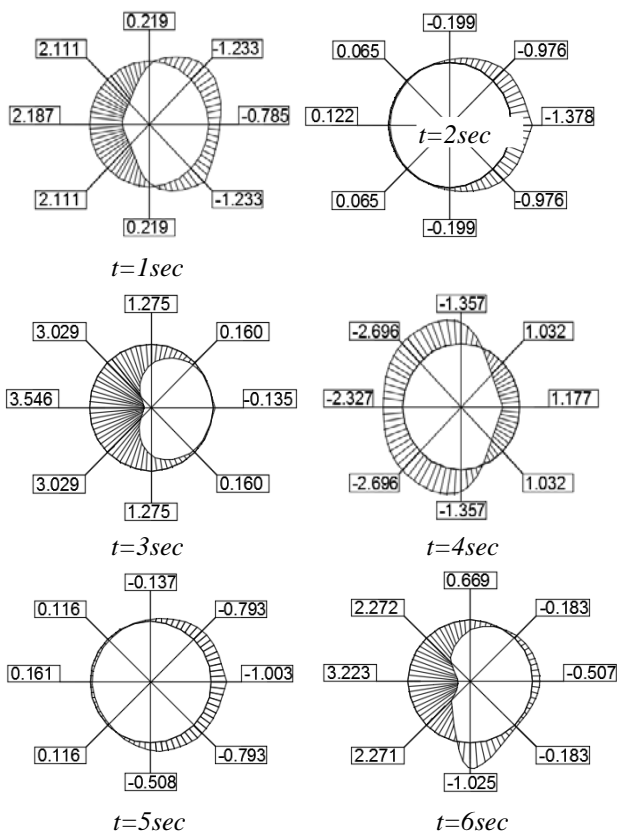


Figure 5. The pressure (KN/m^2) distribution on Cylindrical structure surface at level -5m

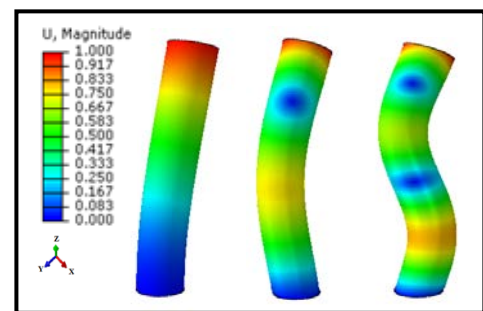
The hydrodynamic wave pressures are calculated by CFD analysis as exemplified in Figure 5. As can be seen in Figure 5., when positive pressure (towards the centre) values are obtained at the front of structure, negative pressure (under pressure) values are observed on structure behind.

Hydrodynamic forces that are transferred from fluid to structure are determined by analysis program [11] according to these hydrodynamic pressures. The natural frequency values and vibration modes are computed by eigenvalue analysis. The FEM model is used to obtain natural frequency values by modal analysis [20]. The first three natural frequency values are listed in Table 1.

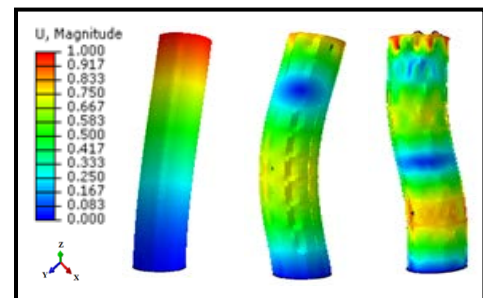
Table 1. The first three natural frequency values

Modes	Cases	Natural frequency (Hz)	Cases	Natural Frequency(Hz)
1th mode	Case I	9.567	Case II	8.381
	Case II	8.381	Case I	9.567
2nd mode	Case I	45.845	Case II	42.515
	Case II	42.515	Case I	45.845
3rd mode	Case I	101.970	Case II	85.751
	Case II	85.751	Case I	101.970

The dominant vibration modes are compared to investigate the design effects on large offshore structures, as shown in Figure 6. There is a predominance of translational displacements towards the “x” axis in the first vibration mode. The third mode happens as a torsion form.



(a) Case I



(b) Case II

Figure 6. First three vibration modes of cylindrical offshore structure

Maximum Von-Misses stress values are $25.28 \times 10^4 \text{ KN/m}^2$ for Case I, and $7.36 \times 10^4 \text{ KN/m}^2$ for Case II while $t_w = 0.003 \text{ m}$.

It has been observed that stress values on structure surface are getting higher closer to the seabed. As expected, the stress values are getting decreased while the wall thicknesses values are increasing.

The Von-Misses stress values of $5.42 \times 10^4 \text{ KN/m}^2$ and $2.39 \times 10^4 \text{ KN/m}^2$ are obtained for Case I and Case II respectively while $t_w = 0.010 \text{ m}$. The stress distribution depending on the wall thickness can be seen in Figure 7. for each case at level -5m when $t = 3s$.

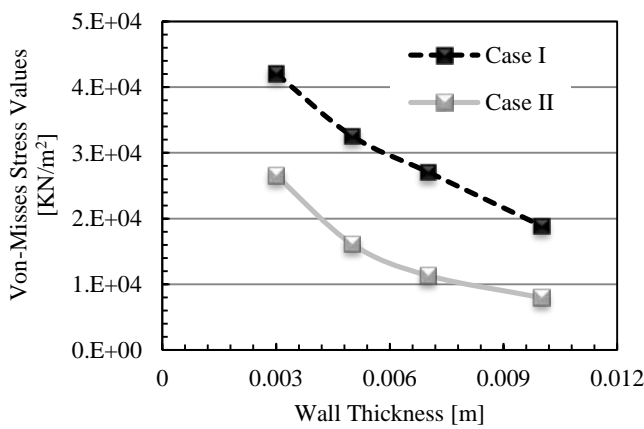
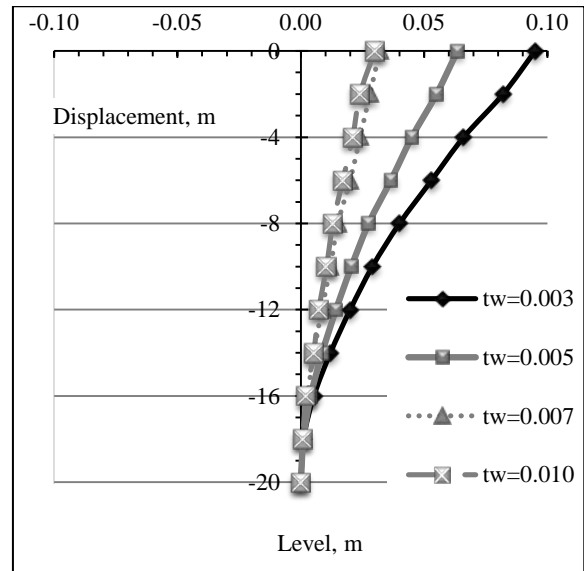


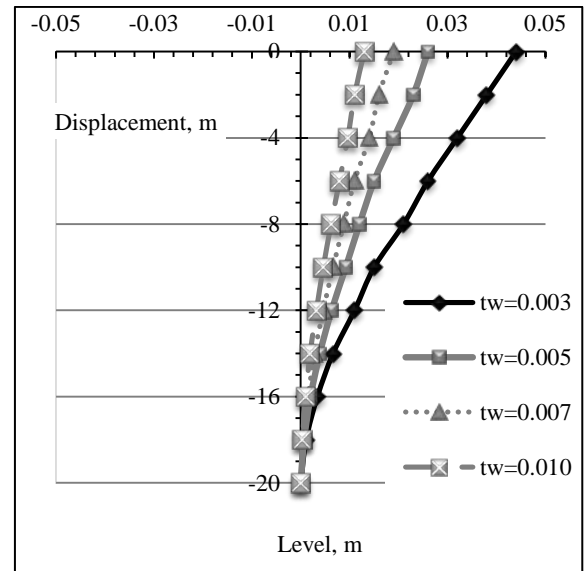
Figure 7. The stress distribution depending on the wall thickness at level -5m when $t = 3s$

As shown in Figure 7., a change in the structural design induces the same magnitude change for responses.

Maximum displacement values are attained at the top of the large cylindrical structures. The maximum values are obtained as 0.095m for Case I when $t = 6s$ and 0.044m for Case II when $t = 1s$ at level 60m as given in Figure 8.



(a) Case I



(b) Case II

Figure 8. The distribution of maximum displacement values

Figure 9a. shows a comparison of the maximum bending moment values along cylindrical structure. The critical values of shear force are determined by evaluating all types of structure and presented in Figure 9b.

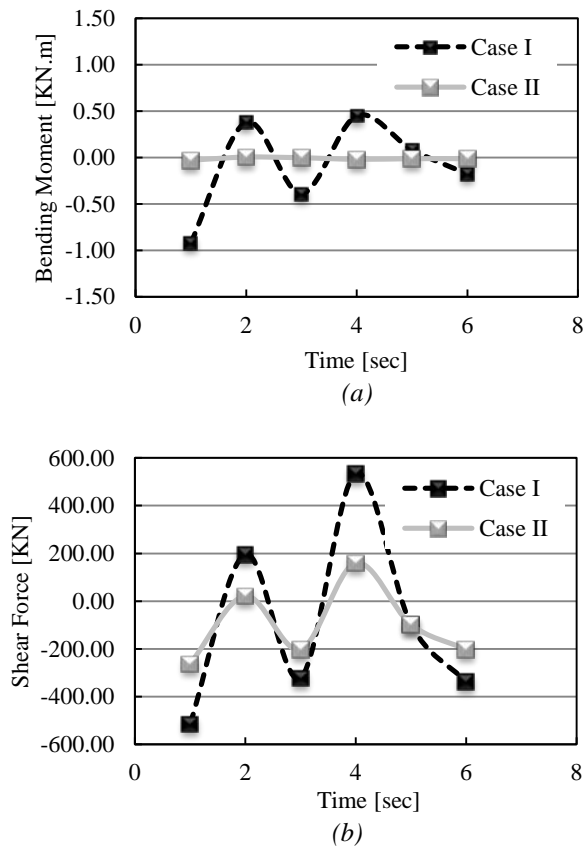


Figure 9. (a) The maximum bending moment variation
(b) The maximum shear force variation

The maximum value is obtained as -0.92KN.m for Case I and -0.028KN.m for Case II. As expected the maximum value occurs at the top of the structures.

Figures 10. and 11. show a comparison of the reaction forces versus the wave period. When the structures are investigated according to reaction forces, the maximum results are obtained from Case I while $t_w=0.003m$.

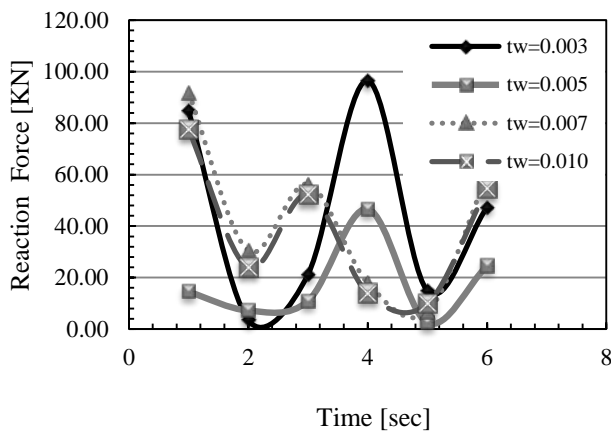


Figure 10. The distribution of reaction force values for Case I

As shown in Figure 10. the maximum value of reaction force is determined as 96.50KN for Case I when $t = 4s$.

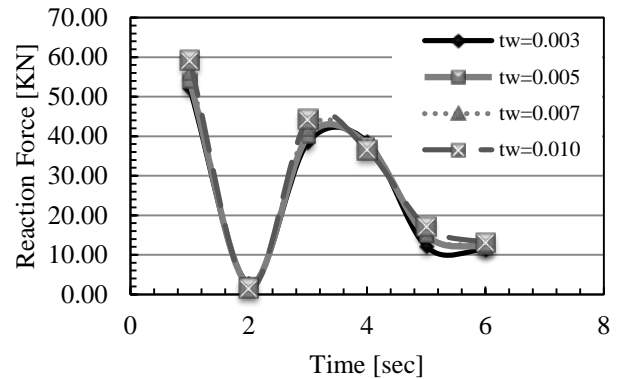


Figure 11. The distribution of reaction force values for Case II

On the other hand, the analysis results for Case II show that the wall thickness has a slight effect on the reaction forces (Figure 11). The maximum value is obtained as 59.19KN when $t = 1s$.

4. Conclusions

In this study the behavior of large cylindrical offshore structures have been investigated which are subjected to wave loads. The wave load distribution is computed by Diffraction Theory. Two different cases of structural model are considered to generate effective design via a nonlinear numerical model using the ABAQUS analysis program. Two-way FSI simulation is utilized to achieve dynamic behavior. To verify the effect of wall thickness on structural behavior, four values of $t_w=0.003, 0.005, 0.007$ and $0.010m$ are assumed. Eight numerical analyses are performed by matching two different structural models with four different wall thickness values. Behavior of various types of offshore structures are evaluated and compared according to the significant stresses and displacements. Significant reductions of displacements and stresses are obtained under diffracted wave loadings. When the displacement values were investigated, it was established that higher values are obtained from Case I. The displacement responses decrease as the model (Case II) is strengthened by steel plates and this reduction reaches at maximum 53.68%. While the value of wall thickness is kept constant, the propagation of stress can be seen more clearly in Case I when compared to Case II. When structures are investigated according to Von-Mises stresses, the highest values of stress results due to strain are obtained for Case I. Hydrodynamic forces decrease due to the wave

velocity closer to the seabed. At that case the maximum values of shear force and bending moment occur at the bottom of cylindrical structure. The maximum shear force values obtained for Case I are decreased by 7% by increasing the wall thickness.

The results indicate that the wall thickness plays a protective role on stability. The reaction force values decrease by 38.67% due to the structural design. When the stress and displacement values are considered, it is observed that Case II is more stable design and provides the optimum conditions. Case II can resist against extreme wave forces which is expected to be encountered during its life span. The results of this study highlight the importance of safe and effective design of large cylindrical offshore structures under hydrodynamic forces.

References

- [1]. Council, G. W. E. (2013). Global wind statistics 2012. *Global Wind Report*.
- [2]. Kurian, V.J., Ng, C.Y., Liew, M.S. (2013). Dynamic responses of truss spar due to wave actions, *Research Journal of Applied Sciences, Engineering and Technology*, 5(3): 812-818
- [3]. Bosma, B. (2014). *On the design, modeling, and testing of ocean wave energy converters*, PhD thesis, Department of Electrical and Computer Engineering, Oregon State University.
- [4]. Chakrabarti, S. K. (1987). *Hydrodynamics of offshore structures*. WIT press.
- [5]. Mansouri, R. & Hadidi, H. (2009). Comprehensive study on the linear hydrodynamic analysis of a truss spar in random waves, *World Acad. Sci. Eng. Technol.*, 53: 930-942.
- [6]. Gücüyen, E. (2017). Analysis of offshore wind turbine tower under environmental loads. *Ships and Offshore Structures*, 12(4), 513-520.
- [7]. Dassault Systemes. (2010a). *Introduction to ABAQUS/CFD*, Velizy-Villacoublay Cedex.
- [8]. Gucuyen, E., Erdem, R.T., Gokkus, U. (2011). Effect of changes on joint connections of steel lattice towers due to environmental loads, *Int J Eng Ind*. 2(1),30-36.
- [9]. Wang, X. (2013). Eulerian–Eulerian solid-liquid two-phase flow of sandstone wastewater in a hydropower station rectangular sedimentation tank, *Eur J Environ Civil Eng*. 17(8):700-719.
- [10]. Passon, P., Branner, K.. (2016). Condensation of long-term wave climates for the fatigue design of hydrodynamically sensitive offshore wind turbine support structures, *Ships Offshore Struct.*, 11(2),142-166.
- [11]. Dassault Systemes, (2010b). *ABAQUS/CAE Version 6.10*, Velizy-Villacoublay Cedex.
- [12]. Lee, M. M. K. (1999). Strength, stress and fracture analyses of offshore tubular joints using finite elements. *Journal of Constructional Steel Research*, 51(3), 265-286.
- [13]. Ergin, A. (2010). *Coastal engineering*, Metu Press.
- [14]. Engineers, U. A. C. O. (2002). Coastal engineering manual. *Engineer Manual*, 1110, 2-1100.
- [15]. Sorensen, R. M. (2005). *Basic coastal engineering* (Vol. 10). Springer Science & Business Media.
- [16]. Samui, P., Chakraborty, S., Kim, D. (2017). *Modeling and simulation techniques in structural engineering*, IGI Global, USA
- [17]. Yang, C., & Ertekin, R. C. (1992). Numerical simulation of nonlinear wave diffraction by a vertical cylinder. *ASME J. Offshore Mech. Arct. Eng*, 114, 36-44.
- [18]. Simao, M., Rodriguez, M., Ramos, A.M. (2015). Computational dynamic models and experiments in the fluid–structure interaction of pipe systems, *Canadian Journal of Civil Engineering*, 43(1): 60-72.
- [19]. Kumar, P.S., Vendhan, C.P., Krishnankutty, P. (2017). Study of water wave diffraction around cylinders using a finite element model of fully nonlinear potential flow theory, *Ships and Offshore Structures*, 12(2): 276-289.
- [20]. Beliveau, J.G. (2003). Dynamics of structures, *Canadian Journal of Civil Engineering*, 30(2):484-485.